



A posteriori analysis of the Newton method applied to the Navier–Stokes problem

Jad Dakroub¹ · Joanna Faddoul² · Toni Sayah²

Received: 7 November 2019 / Published online: 13 February 2020
© Korean Society for Informatics and Computational Applied Mathematics 2020

Abstract

In this paper we study the a posteriori error estimates for the Navier–Stokes equations. The problem is discretized using the finite element method and solved using the Newton iterative algorithm. A posteriori error estimate has been established based on two types of error indicators. Finally, numerical experiments and comparisons with previous works validate the proposed scheme and show the effectiveness of the studied algorithm.

Keywords A posteriori error estimation · Navier–Stokes problem · Finite element method · Newton iterative method

Mathematics Subject Classification 65N30 · 65N15 · 65J15 · 76D05 · 49M15

1 Introduction

Let Ω be a connected open domain in \mathbf{R}^d , $d = 2, 3$, with a Lipschitz continuous boundary $\partial\Omega$. We consider, for a positive constant viscosity ν , the following system:

$$\begin{aligned} -\nu\Delta\mathbf{u} + (\mathbf{u} \cdot \nabla)\mathbf{u} + \nabla p &= \mathbf{f} && \text{in } \Omega \\ \operatorname{div} \mathbf{u} &= 0 && \text{in } \Omega \\ \mathbf{u} &= \mathbf{0} && \text{on } \partial\Omega, \end{aligned} \quad (1.1)$$

✉ Joanna Faddoul
joanna.faddoul@net.usj.edu.lb

Jad Dakroub
jad.dakroub@usj.edu.lb

Toni Sayah
toni.sayah@usj.edu.lb

¹ Faculté des ingénieurs, Université Saint-Joseph de Beyrouth, Beirut, Lebanon

² Laboratoire de mathématiques et applications, Unité de recherche Mathématiques et modélisation, Faculté des sciences, Université Saint-Joseph de Beyrouth, Beirut, Lebanon

where the unknowns are the velocity \mathbf{u} and the pressure p of the fluid. The right-hand side \mathbf{f} belongs to $H^{-1}(\Omega)^d$, the dual of the Sobolev space $H_0^1(\Omega)^d$.

Using \mathcal{P}_1 Lagrange finite elements for the pressure and \mathcal{P}_1 -bubble Lagrange finite elements for the velocity, the discrete variational problem amounts to a system of nonlinear equations. In order to solve it we propose an iterative Newton algorithm which consists at each iteration to solve a linearized problem. We establish the corresponding a posteriori error estimates. Thus, two sources of error appear, due to linearization and discretization. Finally, we perform numerical results that are compared with previous works to show the effectiveness of proposed algorithm.

Many references use the Newton method for the finite element method applied to the Navier–Stokes system, we can cite for instance [12,21,25] and the references inside.

The a posteriori analysis controls the overall discretization error of a problem by providing error indicators easy to compute. Once these error indicators are constructed, their efficiency can be proven by bounding each indicator by the local error. This analysis was first introduced by Babuška [3], and developed by Verfürth [26]. The present work investigates a posteriori error estimates of the finite element discretization of the Navier–Stokes equations in polygonal domains. In fact, many works have been carried out in this field. In [10], El Akkad, El Khalfi and Guessous proposed a numerical solution of the incompressible Navier–Stokes equations based on an algorithm of discretization by mixed finite elements with a posteriori error estimation of the computed solutions. Other works for the a posteriori estimation of stationary Navier–Stokes have been introduced in [19], [20] and [24]. In [6], Bernardi, Hecht and Verfürth considered a variational formulation of the three-dimensional Navier–Stokes equations with mixed boundary conditions and they proved that it admits a solution if the domain satisfies a suitable regularity assumption. In addition, they established *a priori* and a posteriori error estimates. As well, in [16], Ervin, Layton and Maubach present locally calculable a posteriori error estimators for the basic two-level discretization of the Navier–Stokes equations. In some situations and problems, the a posteriori error estimates is based on linearization and discretization errors in the context of an adaptive procedure. This type of analysis was introduced by Chaillou and Suri [8,9] for a general class of problems characterized by strongly monotone operators. It had been developed by El Alaoui, Ern and Vohralík [11] and by Ern and Vohralík [13], for a class of second-order monotone quasi-linear diffusion-type problems approximated by piecewise affine, continuous finite elements.

In [5], We discretized and linearized the problem using an iterative method called the fixed-point algorithm, established corresponding a posteriori error estimates and showed numerical investigations for academic application and the Lid-Driven cavity test. In this paper, we discretise and linearize Navier–Stokes system using the Newton iterative method, establish the corresponding a posteriori error estimates and show that this method is more efficient than the fixed-point one (introduced in [5]) in term of CPU time of computation specially for the Lid-Driven cavity test. In fact, it is well known that the convergence of the Newton method depends on the initial guess but in our applications, a specific treatment is introduced to overcome this difficulty.

The outline of the paper is as follows. In Sect. 2, we present the variational formulation of Navier–Stokes problem (1.1). We introduce in Sect. 3 the discrete variational

problem. The Newton iterative algorithm is presented in Sect. 4. A posteriori analysis of the iterative algorithm is performed in Sect. 5. Section 6 is devoted to the numerical experiments.

2 Preliminaries

We describe in this section the Navier–Stokes problem (1.1) together with its variational formulation. First of all, we recall the main notion and results which we use later on. For the domain Ω , denote by $L^p(\Omega)$ the space of measurable functions v such that $|v|^p$ is integrable. For $v \in L^p(\Omega)$, the norm is defined by

$$\| v \|_{L^p(\Omega)} = \left(\int_{\Omega} |v(x)|^p d\mathbf{x} \right)^{1/p}.$$

We consider the following space

$$X = H_0^1(\Omega)^d = \left\{ \mathbf{v} = (v_i) \in L^2(\Omega)^d; \nabla v_i \in L^2(\Omega)^d; \mathbf{v}|_{\partial\Omega} = 0 \right\},$$

and its dual space $H^{-1}(\Omega)^d$.

We denote by $L_0^2(\Omega)$ the space of functions in $L^2(\Omega)$ with zero mean-value on Ω .

$$M = L_0^2(\Omega) = \left\{ q \in L^2(\Omega); \int_{\Omega} q d\mathbf{x} = 0 \right\}.$$

We recall the Sobolev imbeddings (see Adams [1], Chapter 3).

Lemma 2.1 *For all $j \leq 6$ and $d = 2, 3$, there exists a positive constant S_j such that*

$$\forall v \in H_0^1(\Omega), \quad \| v \|_{L^j(\Omega)} \leq S_j |v|_{1,\Omega}. \tag{2.1}$$

We now assume that the data \mathbf{f} belongs to $H^{-1}(\Omega)^d$. Then the system (1.1) is equivalent to the following variational problem:

Find $\mathbf{u} \in X, p \in M$ such that

$$\begin{aligned} \forall \mathbf{v} \in X, \quad a(\mathbf{u}, \mathbf{v}) + c(\mathbf{u}; \mathbf{u}, \mathbf{v}) + b(\mathbf{v}, p) &= \langle \mathbf{f}, \mathbf{v} \rangle, \\ \forall q \in M, \quad b(\mathbf{u}, q) &= 0, \end{aligned} \tag{2.2}$$

where the bilinear forms $a(., .)$ and $b(., .)$ and the trilinear form $c(., ., .)$ are defined by

$$\begin{aligned}
 a(\mathbf{u}, \mathbf{v}) &= \nu \int_{\Omega} \nabla \mathbf{u} \nabla \mathbf{v} \, d\mathbf{x}, \\
 b(\mathbf{v}, q) &= - \int_{\Omega} q \operatorname{div} \mathbf{v} \, d\mathbf{x}, \\
 c(\mathbf{w}; \mathbf{u}, \mathbf{v}) &= \int_{\Omega} (\mathbf{w} \cdot \nabla) \mathbf{u} \mathbf{v} \, d\mathbf{x}.
 \end{aligned}
 \tag{2.3}$$

Furthermore, the bilinear form $b(\cdot, \cdot)$ satisfies the following inf-sup condition (see [17], Chapter I, Equation (5.14) for instance)

$$\inf_{q \in M, q \neq 0} \sup_{\mathbf{v} \in X} \frac{b(\mathbf{v}, q)}{\|\mathbf{v}\|_X \|q\|_M} = \beta > 0.
 \tag{2.4}$$

The existence and the conditional uniqueness of the solution (\mathbf{u}, p) of problem (2.2) is given in [17] (Chapter IV, Section 2). Furthermore, the solution of the problem (2.2) verify the bound:

$$\|\mathbf{u}\|_{1,\Omega} \leq \frac{c}{\nu} \|\mathbf{f}\|_{-1,\Omega}.
 \tag{2.5}$$

In order to calculate the a posteriori error estimate, we introduce the Stokes equations which are defined as follows:

$$\begin{aligned}
 -\nu \Delta \mathbf{u} + \nabla p &= \mathbf{f} \text{ in } \Omega \\
 \operatorname{div} \mathbf{u} &= 0 \quad \text{in } \Omega \\
 \mathbf{u} &= \mathbf{0} \quad \text{on } \partial\Omega.
 \end{aligned}
 \tag{2.6}$$

Using the previous notation, the Stokes problem amounts to the following variational form:

Find $\mathbf{u} \in X, p \in M$ such that

$$\begin{aligned}
 \forall \mathbf{v} \in X, \quad a(\mathbf{u}, \mathbf{v}) + b(\mathbf{v}, p) &= \langle \mathbf{f}, \mathbf{v} \rangle, \\
 \forall q \in M, \quad b(\mathbf{u}, q) &= 0.
 \end{aligned}
 \tag{2.7}$$

The existence and the uniqueness of the solution $(\mathbf{u}, p) \in X \times M$ of problem (2.7) is given in [17, Chapter I, Section 5.1].

We introduce the following Stokes operator S :

$$\begin{aligned}
 S : H^{-1}(\Omega)^d &\rightarrow X \times M \\
 \mathbf{f} &\mapsto S\mathbf{f} = (\mathbf{w}, \xi),
 \end{aligned}$$

where (\mathbf{w}, ξ) is the solution of the Stokes problem (2.7). We have then the following bound:

$$\|S\mathbf{f}\|_{X \times M} \leq c \|\mathbf{f}\|_{-1,\Omega},
 \tag{2.8}$$

where c is a positive constant independent of \mathbf{f} .

We define also the function G given by

$$\begin{aligned}
 G : X &\rightarrow H^{-1}(\Omega)^d \\
 \mathbf{w} &\mapsto G(\mathbf{w}) = (\mathbf{w} \cdot \nabla) \mathbf{w} - \mathbf{f}
 \end{aligned}$$

and we introduce the map F on $X \times M$ such that for all $\mathbf{V} = (\mathbf{v}, q)$ we have

$$F(\mathbf{V}) = \mathbf{V} + \mathcal{S}G(\mathbf{v}).$$

Then, Problem (2.2) can be equivalently written as

$$F(\mathbf{U}) = 0, \tag{2.9}$$

where $\mathbf{U} = (\mathbf{u}, p)$.

Remark 2.2 In the sequel, we denote by C a generic constant that can vary from line to line but is always independent of all discretization parameters.

3 Finite element discretization

This section collects some useful notation concerning the discrete setting and the a priori estimate.

We assume that Ω is a polygon when $d = 2$ or polyhedron when $d = 3$, so it can be completely meshed. Now, we describe the discretization space. Let $(\mathcal{T}_h)_h$ be a regular family of triangulations of Ω , which is a set of closed non degenerate triangles or tetrahedra, called elements, satisfying,

- for each h , $\bar{\Omega}$ is the union of all elements of \mathcal{T}_h ;
- the intersection of two distinct elements of \mathcal{T}_h is either empty, a common vertex, or an entire common edge or face;
- the ratio of the diameter of an element K in \mathcal{T}_h to the diameter of its inscribed circle or ball is bounded by a constant independent of h .

As usual, h stands for the maximum of the diameters $h_K, K \in \mathcal{T}_h$.

Let (X_h, M_h) be the couple of discrete spaces corresponding to (X, M) defined as follow :

$$M_h = \left\{ q_h \in M, \forall K \in \mathcal{T}_h, q_{h|_K} \in \mathcal{P}_1(K) \right\} \text{ and}$$

$$X_h = \left\{ \mathbf{v}_h \in X, \forall K \in \mathcal{T}_h, \mathbf{v}_{h|_K} \in (\mathcal{P}_1(K)\text{-bubble})^d \right\}$$

where $\mathcal{P}_1(K)$ stands for the space of restrictions to K of affine functions. $\mathcal{P}_1(K)$ -bubble is the sum of a polynomial of $\mathcal{P}_1(K)$ and a ‘‘bubble’’ function b_K . Denoting the vertices of K by $a_i, 1 \leq i \leq d + 1$, and its corresponding barycentric coordinates by λ_i , the basic bubble function b_K is the polynomial of degree three

$$b_K(x) = \lambda_1(x) \dots \lambda_{d+1}(x).$$

We observe that $b_K(x) = 0$ on ∂K and that $b_K(x) > 0$ on K . The graph of b_K looks like a bubble attached to the boundary of K , hence its name.

We then consider the following finite element discretization of Navier–Stokes problem (2.2), obtained by the Galerkin method:

Find $\mathbf{u}_h \in X_h, p_h \in M_h$ such that

$$\begin{aligned} \forall \mathbf{v}_h \in X_h, \quad & \nu \int_{\Omega} \nabla \mathbf{u}_h \nabla \mathbf{v}_h d\mathbf{x} + \int_{\Omega} (\mathbf{u}_h \cdot \nabla) \mathbf{u}_h \mathbf{v}_h d\mathbf{x} - \int_{\Omega} p_h \operatorname{div} \mathbf{v}_h d\mathbf{x} = \langle \mathbf{f}, \mathbf{v}_h \rangle, \\ \forall q_h \in M_h, \quad & \int_{\Omega} q_h \operatorname{div} \mathbf{u}_h d\mathbf{x} = 0. \end{aligned} \tag{3.1}$$

In order to solve the discrete problem (3.1), we introduce the following space

$$V_h = \left\{ \mathbf{v}_h \in X_h; \forall q_h \in M_h, - \int_{\Omega} q_h \operatorname{div} \mathbf{v}_h d\mathbf{x} = 0 \right\}.$$

Problem (3.1) is then equivalent to the problem:

Find $\mathbf{u}_h \in V_h$ such that

$$\forall \mathbf{v}_h \in V_h, \quad \nu \int_{\Omega} \nabla \mathbf{u}_h \nabla \mathbf{v}_h d\mathbf{x} + \int_{\Omega} (\mathbf{u}_h \cdot \nabla) \mathbf{u}_h \mathbf{v}_h d\mathbf{x} = \langle \mathbf{f}, \mathbf{v}_h \rangle. \tag{3.2}$$

Problem (3.1) can be equivalently written as the following

$$F_h(\mathbf{U}_h) = 0, \tag{3.3}$$

where F_h is a map on $X_h \times M_h$ given by

$$F_h(\mathbf{U}_h) = \mathbf{U}_h + \mathcal{S}_h G(\mathbf{u}_h),$$

such that the operator \mathcal{S}_h is the discrete Stokes operator which associates to each $\mathbf{f} \in H^{-1}(\Omega)^d$ the solution $\mathbf{U}_h = (\mathbf{u}_h, p_h)$ of the following discrete Stokes problem:

$$\left\{ \begin{array}{l} \text{Trouver } \mathbf{u}_h \in X_h, p_h \in M_h \text{ tels que} \\ \forall \mathbf{v}_h \in X_h, \quad \nu \int_{\Omega} \nabla \mathbf{u}_h \nabla \mathbf{v}_h d\mathbf{x} - \int_{\Omega} p_h \operatorname{div} \mathbf{v}_h d\mathbf{x} = \langle \mathbf{f}, \mathbf{v}_h \rangle, \\ \forall q_h \in M_h, \quad \int_{\Omega} q_h \operatorname{div} \mathbf{u}_h d\mathbf{x} = 0. \end{array} \right. \tag{3.4}$$

The discrete Stokes operator \mathcal{S}_h verifies, for each $\mathbf{f} \in H^{-1}(\Omega)^d$, the following bound (see [17]):

$$\| \mathcal{S}_h \mathbf{f} \|_{X \times M} \leq c \| \mathbf{f} \|_{-1, \Omega}. \tag{3.5}$$

Theorem 3.1 [17] *Problem (3.1) admits at least one solution $\mathbf{U}_h = (\mathbf{u}_h, p_h) \in X_h \times M_h$ verifying the estimate*

$$\| \mathbf{U}_h \|_{X \times M} \leq c \| \mathbf{f} \|_{-1, \Omega},$$

where c is a positive constant independent of \mathbf{U}_h . Furthermore, if $\mathbf{u} \in H^2(\Omega)^d$ and $p \in H^1(\Omega)$, we have the following a priori error estimate:

$$\|\mathbf{u} - \mathbf{u}_h\|_{1,\Omega} + \|p - p_h\|_{0,\Omega} \leq Ch,$$

where C is a positive constant independent of h but depends on \mathbf{u} , p and Ω .

For the proof of the previous theorem, we refer to [17] (Chapter 4, Theorem 4.1).

It is well known that the proof of the uniqueness of the solution of Problem (3.1) requires a specific condition and treatment. In fact, either we impose conditions on the data \mathbf{f} called the smallness condition (see [17]), or we allow the existence of several solutions and we decide to discrete the nonsingular solution of (2.2) defined as:

Definition 3.2 We define a nonsingular solution \mathbf{U} of Problem (2.2) by the two conditions:

- (1) $F(\mathbf{U}) = 0$.
- (2) $DF(\mathbf{U})$ is an isomorphism of $X \times M$.

We have the following existence and uniqueness result of the solution of Problem (3.1):

Theorem 3.3 [17] *Let \mathbf{U} be a nonsingular solution of Problem 2.9. Then, there exists a neighborhood \mathcal{O} of \mathbf{U} of radius independent of h and a positive real number h_0 such that for each $h \leq h_0$, Problem (3.3) admits a unique nonsingular solution in \mathcal{O} . Furthermore, if $\mathbf{u} \in H^2(\Omega)^d$ and $p \in H^1(\Omega)$, we have the following a priori error estimate:*

$$\|\mathbf{u} - \mathbf{u}_h\|_{1,\Omega} + \|p - p_h\|_{0,\Omega} \leq Ch,$$

where C is a positive constant independent of h .

4 Newton iterative algorithm

There exist in the literature many iterative algorithms to solve the Navier–Stokes discrete problem. For instance, we refer to [7] for a time dependent discrete problem (even for steady state problem), to [2] for a stabilized finite element method, ... In [5], we study a very simple iterative algorithm which linearizes the discrete problem and starts with an initial guess \mathbf{u}_h^0 . We propose in this section to solve Problem (3.3) by using Newton iterative algorithm, to establish the corresponding a posteriori error estimates and to compare the numerical results with [5].

To compute the solution of the nonlinear problem (3.3), we propose the following Newton algorithm:

$$\begin{cases} \text{Having } \mathbf{u}_h^i \in X_h, \text{ compute } \mathbf{U}_h^{i+1} = (\mathbf{u}_h^{i+1}, q_h^{i+1}) \in X_h \times M_h \text{ such that} \\ DF_h(\mathbf{U}_h^i)(\mathbf{U}_h^{i+1} - \mathbf{U}_h^i) = -F_h(\mathbf{U}_h^i). \end{cases} \tag{4.1}$$

Algorithm (4.1) can be explicitly given by the following:

Let \mathbf{u}_h^0 be an initial guess. We introduce, for $i \geq 0$, the following algorithm:

Find $\mathbf{u}_h^{i+1} \in X_h$, $p_h^{i+1} \in M_h$ such that

$$\begin{aligned} \forall \mathbf{v}_h \in X_h, \quad & \nu \int_{\Omega} \nabla \mathbf{u}_h^{i+1} \nabla \mathbf{v}_h \, d\mathbf{x} + \int_{\Omega} (\mathbf{u}_h^i \cdot \nabla) \mathbf{u}_h^{i+1} \mathbf{v}_h \, d\mathbf{x} + \int_{\Omega} (\mathbf{u}_h^{i+1} \cdot \nabla) \mathbf{u}_h^i \mathbf{v}_h \, d\mathbf{x} \\ & - \int_{\Omega} p_h^{i+1} \operatorname{div} \mathbf{v}_h \, d\mathbf{x} \\ & = \langle \mathbf{f}, \mathbf{v}_h \rangle + \int_{\Omega} (\mathbf{u}_h^i \cdot \nabla) \mathbf{u}_h^i \mathbf{v}_h \, d\mathbf{x}, \\ \forall q_h \in M_h, \quad & \int_{\Omega} q_h \operatorname{div} \mathbf{u}_h^{i+1} \, d\mathbf{x} = 0. \end{aligned} \quad (4.2)$$

We clearly see that problem (4.2) has the following form:

Find $\mathbf{u}_h^{i+1} \in V_h$ such that

$$\begin{aligned} \forall \mathbf{v}_h \in V_h, \quad & \nu \int_{\Omega} \nabla \mathbf{u}_h^{i+1} \nabla \mathbf{v}_h \, d\mathbf{x} + \int_{\Omega} (\mathbf{u}_h^i \cdot \nabla) \mathbf{u}_h^{i+1} \mathbf{v}_h \, d\mathbf{x} + \int_{\Omega} (\mathbf{u}_h^{i+1} \cdot \nabla) \mathbf{u}_h^i \mathbf{v}_h \, d\mathbf{x} \\ & = \langle \mathbf{f}, \mathbf{v}_h \rangle + \int_{\Omega} (\mathbf{u}_h^i \cdot \nabla) \mathbf{u}_h^i \mathbf{v}_h \, d\mathbf{x}. \end{aligned} \quad (4.3)$$

Remark 4.1 In [5], we have introduced the following algorithm

$$\begin{aligned} \forall \mathbf{v}_h \in X_h, \quad & \nu \int_{\Omega} \nabla \mathbf{u}_h^{i+1} \nabla \mathbf{v}_h \, d\mathbf{x} + \int_{\Omega} (\mathbf{u}_h^i \cdot \nabla) \mathbf{u}_h^{i+1} \mathbf{v}_h \, d\mathbf{x} - \int_{\Omega} p_h^{i+1} \operatorname{div} \mathbf{v}_h \, d\mathbf{x} = \langle \mathbf{f}, \mathbf{v}_h \rangle, \\ \forall q_h \in M_h, \quad & \int_{\Omega} q_h \operatorname{div} \mathbf{u}_h^{i+1} \, d\mathbf{x} = 0. \end{aligned} \quad (4.4)$$

The convergence properties of (4.4) and of more sophisticated linearization algorithms have been proved, see [4] among others. For instance, the convergence is faster for the Newton's algorithm (4.2), but it only holds for a very accurate choice of the initial value (even solving a Stokes problem as an initial step can lead to a divergence of the algorithm for high values of the Reynolds number, i.e. when the solution of the Navier–Stokes is not unique, see [22, Section 4.3.1]). We will see in the last section that we can overcome this difficulty by a specific technique when we show numerical results for the cavity problem.

Remark 4.2 The following technics of a posteriori error estimates based on two types of indicators (discretization and linearization) can be followed for almost iterative algorithm.

To prove the existence and uniqueness of the solution of Problem (4.2), we shall introduce the following two lemmas:

Lemma 4.3 $DF_h(\mathbf{V}_h)$ is Lipschitz-continuous with respect to \mathbf{V}_h and for each $\mathbf{U}_h = (\mathbf{u}_h, p_h)$ and $\mathbf{V}_h = (\mathbf{v}_h, q_h)$ in $X_h \times M_h$, there exists $K > 0$ such that

$$\| DF_h(\mathbf{U}_h) - DF_h(\mathbf{V}_h) \|_{\mathcal{L}(X_h \times M_h)} \leq K \| \mathbf{U}_h - \mathbf{V}_h \|_{X_h \times M_h}.$$

Proof For all $\mathbf{U}_h = (\mathbf{u}_h, p_h)$ and $\mathbf{V}_h = (\mathbf{v}_h, q_h)$ in $X_h \times M_h$, We have

$$\| DF_h(\mathbf{U}_h) - DF_h(\mathbf{V}_h) \|_{\mathcal{L}(X_h \times M_h)} = \| S_h(DG(\mathbf{u}_h) - DG(\mathbf{v}_h)) \|_{\mathcal{L}(X_h \times M_h)}. \tag{4.5}$$

By using (3.5), we get for all $\mathbf{z}_h \in X_h$ the following bound:

$$\| S_h(DG(\mathbf{u}_h) \cdot \mathbf{z}_h - DG(\mathbf{v}_h) \cdot \mathbf{z}_h) \|_{X_h \times M_h} \leq c \| DG(\mathbf{u}_h) \cdot \mathbf{z}_h - DG(\mathbf{v}_h) \cdot \mathbf{z}_h \|_{-1, \Omega}. \tag{4.6}$$

We observe that

$$DG(\mathbf{u}_h) \cdot \mathbf{z}_h - DG(\mathbf{v}_h) \cdot \mathbf{z}_h = \mathbf{z}_h \cdot \nabla(\mathbf{u}_h - \mathbf{v}_h) + (\mathbf{u}_h - \mathbf{v}_h) \cdot \nabla \mathbf{z}_h, \tag{4.7}$$

hence

$$\| (DG(\mathbf{u}_h) - DG(\mathbf{v}_h)) \cdot \mathbf{z}_h \|_{-1, \Omega} \leq 2S_4^2 |\mathbf{u}_h - \mathbf{v}_h|_{1, \Omega} |\mathbf{z}_h|_{1, \Omega}. \tag{4.8}$$

Thus, combining (4.5), (4.6) and (4.8) yields the desired property. □

Lemma 4.4 [17] *Let $\mathbf{U}_h = (\mathbf{u}_h, p_h)$ be a nonsingular solution of Problem (3.3) and let $\mathbf{V}_h = (\mathbf{v}_h, q_h) \in X_h \times M_h$, we define*

$$\begin{aligned} \gamma_h &= \| \{DF_h(\mathbf{U}_h)\}^{-1} \|_{\mathcal{L}(X_h \times M_h)}, \\ \mu_h &= \| DF_h(\mathbf{U}_h) - DF_h(\mathbf{V}_h) \|_{\mathcal{L}(X_h \times M_h)}. \end{aligned}$$

Then, under the condition $\gamma_h \mu_h < 1$, $DF_h(\mathbf{V}_h)$ is an isomorphism of $X_h \times M_h$ and we have

$$\| \{DF_h(\mathbf{V}_h)\}^{-1} \|_{\mathcal{L}(X_h \times M_h)} \leq \frac{\gamma_h}{1 - \gamma_h \mu_h}.$$

The previous two lemmas allows us to get the existence, uniqueness and the convergence of the solution of Problem (4.2):

Theorem 4.5 *Let $\mathbf{U}_h = (\mathbf{u}_h, p_h)$ be a nonsingular solution of Problem (3.3). There exists a positive real number α such that for each initial guess \mathbf{U}_h^0 in the ball $B(\mathbf{U}_h, \alpha)$ of center \mathbf{U}_h and radius α , the algorithm (4.2) admits a unique solution $\mathbf{U}_h^{n+1} \in B(\mathbf{U}_h, \alpha)$ which converges to \mathbf{U}_h .*

Proof Lemma 4.3 deduces that $DF_h(\mathbf{V}_h)$ is Lipschitz-continuous with respect to \mathbf{V}_h and for each $\mathbf{U}_h = (\mathbf{u}_h, p_h)$ and $\mathbf{V}_h = (\mathbf{v}_h, q_h)$ in $\in X_h \times M_h$, there exists a real $K > 0$ such that

$$\| DF_h(\mathbf{u}_h) - DF_h(\mathbf{v}_h) \|_{\mathcal{L}(X_h \times M_h)} \leq K \| \mathbf{U}_h - \mathbf{V}_h \|_{X_h \times M_h}.$$

Let \mathbf{U}_h be a nonsingular solution of (3.3) and $\mathbf{V}_h \in X_h \times M_h$. By introducing the following variables of Lemma 4.4:

$$\begin{aligned} \gamma_h &= \| \{DF_h(\mathbf{U}_h)\}^{-1} \|_{\mathcal{L}(X_h \times M_h)}, \\ \mu_h &= \| DF_h(\mathbf{U}_h) - DF_h(\mathbf{V}_h) \|_{\mathcal{L}(X_h \times M_h)}, \end{aligned}$$

we get

$$\gamma_h \mu_h \leq \gamma_h K \|\mathbf{U}_h - \mathbf{V}_h\|_{X_h \times M_h}$$

and then for each $\mathbf{V}_h \in B(\mathbf{U}_h, \alpha)$ for $\alpha \leq \frac{1}{2\gamma_h K}$, we have:

$$\begin{aligned} \gamma_h \mu_h &\leq \gamma_h K \|\mathbf{U}_h - \mathbf{V}_h\|_{X_h \times M_h} \\ &\leq \gamma_h K \alpha \\ &\leq \frac{1}{2}. \end{aligned}$$

Then by applying Lemma 4.4 we get the following bound:

$$\begin{aligned} \|\{DF_h(\mathbf{V}_h)\}^{-1}\|_{\mathcal{L}(X_h \times M_h)} &\leq \frac{\gamma_h}{1 - \gamma_h \mu_h} \\ &\leq 2\gamma_h. \end{aligned}$$

On the other hand, we consider Algorithm (4.2) where the initial guess $\mathbf{U}_h^0 \in B(\mathbf{U}_h, \alpha)$. We proceed by induction: for $\mathbf{U}_h^n \in B(\mathbf{U}_h, \alpha)$, $\{DF_h(\mathbf{U}_h^n)\}^{-1}$ exists and we have

$$\begin{aligned} \mathbf{U}_h^{n+1} - \mathbf{U}_h &= \mathbf{U}_h^n - \mathbf{U}_h + \{DF_h(\mathbf{U}_h^n)\}^{-1} \cdot (F_h(\mathbf{U}_h) - F_h(\mathbf{U}_h^n)) \\ &= \{DF_h(\mathbf{U}_h^n)\}^{-1} \int_0^1 [DF_h(\mathbf{U}_h^n + t(\mathbf{U}_h - \mathbf{U}_h^n)) - DF_h(\mathbf{U}_h^n)] \\ &\quad \times (\mathbf{U}_h - \mathbf{U}_h^n) dt. \end{aligned}$$

Lemma 4.3 gives

$$\begin{aligned} \|\mathbf{U}_h^{n+1} - \mathbf{U}_h\|_{X_h \times M_h} &\leq \gamma_h K \|\mathbf{U}_h^n - \mathbf{U}_h\|_{X_h \times M_h} \\ &\leq \frac{1}{2} \|\mathbf{U}_h^n - \mathbf{U}_h\|_{X_h \times M_h}. \end{aligned}$$

Consequently, \mathbf{U}_h^{n+1} is in the ball $B(\mathbf{U}_h, \alpha)$ and the sequence \mathbf{U}_h^n converges to \mathbf{U}_h . \square

In what follows, for simplicity reasons, we suppose $d = 2$. In fact, this work can easily be extended to $d = 3$ but requires some more technicalities.

5 A posteriori error analysis

We start this section by introducing some additional notation needed for constructing and analyzing the error indicators in the sequel.

For any element $K \in \mathcal{T}_h$ we denote by $\mathcal{E}(K)$ the set of its edges and we set

$$\mathcal{E}_h = \bigcup_{K \in \mathcal{T}_h} \mathcal{E}(K).$$

With any edge $e \in \mathcal{E}_h$ we associate a unit vector \mathbf{n} such that \mathbf{n} is orthogonal to e . We split $\mathcal{E}(K)$ in the form

$$\mathcal{E}(K) = \mathcal{E}_{K, \partial\Omega} \cup \mathcal{E}_{K, \Omega},$$

where $\mathcal{E}_{K, \partial\Omega}$ is the set of edges in $\mathcal{E}(K)$ that lie on $\partial\Omega$ and $\mathcal{E}_{K, \Omega} = \mathcal{E}(K) \setminus \mathcal{E}_{K, \partial\Omega}$. Furthermore, for $K \in \mathcal{T}_h$ and $e \in \mathcal{E}_h$, let h_K and h_e be their diameter and length respectively. An important tool in the construction of bounds for the total error is Clément’s interpolation operator \mathcal{R}_h with values in X_h . The operator \mathcal{R}_h satisfies, for all $v \in H_0^1(\Omega)$, the following local approximation properties (see Verfürth, [26], Chapter 1):

$$\begin{aligned} \|v - \mathcal{R}_h v\|_{L^2(K)} &\leq Ch_K |v|_{1, \Delta_K}, \\ \|v - \mathcal{R}_h v\|_{L^2(e)} &\leq Ch_e^{1/2} |v|_{1, \Delta_e}, \end{aligned}$$

where Δ_K and Δ_e are the following sets:

$$\Delta_K = \bigcup \left\{ K' \in \mathcal{T}_h; K' \cap K \neq \emptyset \right\} \quad \text{and} \quad \Delta_e = \bigcup \left\{ K' \in \mathcal{T}_h; K' \cap e \neq \emptyset \right\}.$$

We now recall the following properties (see Verfürth, [26], Chapter 1): Let r be a positive integer. For all $v \in P_r(K)$, the following properties hold

$$C \|v\|_{L^2(K)} \leq \|vb_K^{1/2}\|_{L^2(K)} \leq \|v\|_{L^2(K)} \tag{5.1}$$

$$|v|_{1, K} \leq Ch_K^{-1} \|v\|_{L^2(K)}, \tag{5.2}$$

where b_K is the bubble function of the element K .

Finally, we denote by $[v_h]$ the jump of v_h across the common edge e of two adjacent elements $K, K' \in \mathcal{T}_h$. We have now provided all prerequisites to establish bounds for the total error.

We start the a posteriori analysis of the iterative algorithm. In order to prove an upper bound of the error, we first introduce an approximation \mathbf{f}_h of the data \mathbf{f} which is constant on each element K of \mathcal{T}_h . Then, we distinguish the discretization and linearization errors. We first write the weak residual equation.

Let (\mathbf{u}, p) and (\mathbf{u}_h^i, p_h^i) be the solutions of (2.2) and (4.2), for all $\mathbf{v} \in X$ and $\mathbf{v}_h \in X_h$, we have:

$$\begin{aligned}
 & \nu \int_{\Omega} \nabla \mathbf{u} \nabla \mathbf{v} \, d\mathbf{x} + \int_{\Omega} (\mathbf{u} \cdot \nabla) \mathbf{u} \mathbf{v} \, d\mathbf{x} - \int_{\Omega} p \operatorname{div} \mathbf{v} \, d\mathbf{x} - \nu \int_{\Omega} \nabla \mathbf{u}_h^{i+1} \nabla \mathbf{v} \, d\mathbf{x} \\
 & \quad - \int_{\Omega} (\mathbf{u}_h^i \cdot \nabla) \mathbf{u}_h^{i+1} \mathbf{v} \, d\mathbf{x} - \int_{\Omega} (\mathbf{u}_h^{i+1} \cdot \nabla) \mathbf{u}_h^i \mathbf{v} \, d\mathbf{x} + \int_{\Omega} (\mathbf{u}_h^i \cdot \nabla) \mathbf{u}_h^i \mathbf{v} \, d\mathbf{x} + \int_{\Omega} p_h^{i+1} \operatorname{div} \mathbf{v} \, d\mathbf{x} \\
 & = \langle \mathbf{f}, \mathbf{v} - \mathbf{v}_h \rangle - \nu \int_{\Omega} \nabla \mathbf{u}_h^{i+1} \nabla (\mathbf{v} - \mathbf{v}_h) \, d\mathbf{x} - \int_{\Omega} (\mathbf{u}_h^i \cdot \nabla) \mathbf{u}_h^{i+1} (\mathbf{v} - \mathbf{v}_h) \, d\mathbf{x} \\
 & \quad - \int_{\Omega} (\mathbf{u}_h^{i+1} \cdot \nabla) \mathbf{u}_h^i (\mathbf{v} - \mathbf{v}_h) \, d\mathbf{x} + \int_{\Omega} (\mathbf{u}_h^i \cdot \nabla) \mathbf{u}_h^i (\mathbf{v} - \mathbf{v}_h) \, d\mathbf{x} + \int_{\Omega} p_h^{i+1} \operatorname{div} (\mathbf{v} - \mathbf{v}_h) \, d\mathbf{x}.
 \end{aligned} \tag{5.3}$$

Adding and subtracting $\int_{\Omega} (\mathbf{u}_h^{i+1} \cdot \nabla) \mathbf{u}_h^{i+1} \mathbf{v} \, d\mathbf{x}$ and using the Green formula, give

$$\begin{aligned}
 & \nu \int_{\Omega} \nabla \mathbf{u} \nabla \mathbf{v} \, d\mathbf{x} + \int_{\Omega} (\mathbf{u} \cdot \nabla) \mathbf{u} \mathbf{v} \, d\mathbf{x} - \int_{\Omega} p \operatorname{div} \mathbf{v} \, d\mathbf{x} \\
 & \quad - \nu \int_{\Omega} \nabla \mathbf{u}_h^{i+1} \nabla \mathbf{v} \, d\mathbf{x} - \int_{\Omega} (\mathbf{u}_h^{i+1} \cdot \nabla) \mathbf{u}_h^{i+1} \mathbf{v} \, d\mathbf{x} + \int_{\Omega} p_h^{i+1} \operatorname{div} \mathbf{v} \, d\mathbf{x} \\
 & = \sum_{K \in \mathcal{T}_h} \int_K (\mathbf{f} - \mathbf{f}_h) (\mathbf{v} - \mathbf{v}_h) \, d\mathbf{x} + \int_{\Omega} ((\mathbf{u}_h^i - \mathbf{u}_h^{i+1}) \cdot \nabla) \mathbf{u}_h^{i+1} \mathbf{v} \, d\mathbf{x} \\
 & \quad + \int_{\Omega} ((\mathbf{u}_h^{i+1} - \mathbf{u}_h^i) \cdot \nabla) \mathbf{u}_h^i \mathbf{v} \, d\mathbf{x} \\
 & \quad + \sum_{K \in \mathcal{T}_h} \left\{ \int_K (\mathbf{f}_h + \nu \Delta \mathbf{u}_h^{i+1} - (\mathbf{u}_h^i \cdot \nabla) \mathbf{u}_h^{i+1} - (\mathbf{u}_h^{i+1} \cdot \nabla) \mathbf{u}_h^i \right. \\
 & \quad \left. + (\mathbf{u}_h^i \cdot \nabla) \mathbf{u}_h^i - \nabla p_h^{i+1}) (\mathbf{v} - \mathbf{v}_h) \, d\mathbf{x} \right. \\
 & \quad \left. - \frac{1}{2} \sum_{e \in \mathcal{E}_{K,\Omega}} \int_e \left[\nu \frac{\partial \mathbf{u}_h^{i+1}}{\partial n} - p_h^{i+1} \mathbf{n} \right] \cdot (\mathbf{v} - \mathbf{v}_h) \, d\tau \right\}
 \end{aligned} \tag{5.4}$$

where τ denotes the tangential coordinate on ∂K .

On the other hand, for all $q \in L^2(\Omega)$

$$b(\mathbf{u} - \mathbf{u}_h^{i+1}, q) = \int_{\Omega} q \operatorname{div} \mathbf{u}_h^{i+1} \, d\mathbf{x}. \tag{5.5}$$

We now define the local linearization indicator $\eta_{K,i}^{(L)}$ and the local discretization indicator $\eta_{K,i}^{(D)}$, corresponding to an element $K \in \mathcal{T}_h$, by:

$$\eta_{K,i}^{(L)} = |\mathbf{u}_h^{i+1} - \mathbf{u}_h^i|_{1,K}, \tag{5.6}$$

$$\begin{aligned}
 \eta_{K,i}^{(D)} & = h_K \left\| \mathbf{f}_h + \nu \Delta \mathbf{u}_h^{i+1} - (\mathbf{u}_h^i \cdot \nabla) \mathbf{u}_h^{i+1} - (\mathbf{u}_h^{i+1} \cdot \nabla) \mathbf{u}_h^i + (\mathbf{u}_h^i \cdot \nabla) \mathbf{u}_h^i - \nabla p_h^{i+1} \right\|_{L^2(K)} \\
 & \quad + \frac{1}{2} \sum_{e \in \mathcal{E}_{K,\Omega}} h_e^{1/2} \left\| \left[\nu \frac{\partial \mathbf{u}_h^{i+1}}{\partial n} - p_h^{i+1} \mathbf{n} \right] \right\|_{L^2(e)} + \left\| \operatorname{div} \mathbf{u}_h^{i+1} \right\|_{L^2(K)}.
 \end{aligned} \tag{5.7}$$

We can now state the first result of this section:

Theorem 5.1 *Let $\mathbf{U} = (\mathbf{u}, p)$ be a nonsingular solution of Problem (2.2) and $\mathbf{U}_h^{i+1} = (\mathbf{u}_h^{i+1}, p_h^{i+1}) \in X_h \times M_h$ be the solutions of the iterative problem (4.2). Then, there exists a neighborhood \mathcal{O} of \mathbf{U} in X such that any solution \mathbf{U}_h^{i+1} of problem (4.2) in \mathcal{O} satisfies the following a posteriori error estimate*

$$\begin{aligned} \|\mathbf{u} - \mathbf{u}_h^{i+1}\|_{1,\Omega} + \|p - p_h^{i+1}\|_{L^2(\Omega)} &\leq C \left(\sum_{K \in \mathcal{T}_h} ((\eta_{K,i}^{(D)})^2 + h_K^2 \|\mathbf{f} - \mathbf{f}_h\|_{L^2(K)}^2) \right)^{1/2} \\ &+ C' \left(\sum_{K \in \mathcal{T}_h} (\eta_{K,i}^{(L)})^2 \right)^{1/2}. \end{aligned}$$

Proof Let $\mathbf{U} = (\mathbf{u}, p)$ be a nonsingular solution of Problem (2.2) and $\mathbf{U}_h^{i+1} = (\mathbf{u}_h^{i+1}, p_h^{i+1}) \in X_h \times M_h$ be the solutions of the iterative problem (4.2). Owing to Lemma 4.3, it follows from [23] (see also [26, Prop. 2.2]) that, for any \mathbf{U}_h^{i+1} in a appropriate neighborhood \mathcal{O} of \mathbf{U}

$$\|\mathbf{U} - \mathbf{U}_h^{i+1}\|_{X \times M} \leq C \|\mathbf{U}_h^{i+1} + S\mathcal{G}(\mathbf{u}_h^{i+1})\|_{X \times M}. \tag{5.8}$$

By using (2.8), we have

$$\begin{aligned} \|\mathbf{U} - \mathbf{U}_h^{i+1}\|_{X \times M} &\leq C \|\mathcal{S}(\mathcal{S}^{-1}\mathbf{U}_h^{i+1} + G(\mathbf{u}_h^{i+1}))\|_{X \times M} \\ &\leq c C \|\mathcal{S}^{-1}\mathbf{U}_h^{i+1} + G(\mathbf{u}_h^{i+1})\|_{X'}. \end{aligned} \tag{5.9}$$

It follows from the properties of \mathcal{S} and the relations (5.4) and (5.5), that (5.9) can equivalently be written as follow

$$\begin{aligned} \|\mathbf{U} - \mathbf{U}_h^{i+1}\|_{X \times M} &\leq c C \left(\sup_{\substack{\mathbf{v} \in X \\ \mathbf{v} \neq 0}} \frac{\langle \mathbf{f} - \mathbf{f}_h, \mathbf{v} - \mathbf{v}_h \rangle + \langle \mathcal{R}, \mathbf{v} - \mathbf{v}_h \rangle}{|\mathbf{v}|_{1,\Omega}} \right. \\ &+ \sup_{\substack{\mathbf{v} \in X \\ \mathbf{v} \neq 0}} \frac{\int_{\Omega} ((\mathbf{u}_h^{i+1} - \mathbf{u}_h^i) \cdot \nabla) \mathbf{u}_h^i \mathbf{v} \, dx}{|\mathbf{v}|_{1,\Omega}} \\ &\left. + \sup_{\substack{\mathbf{v} \in X \\ \mathbf{v} \neq 0}} \frac{\int_{\Omega} ((\mathbf{u}_h^{i+1} - \mathbf{u}_h^i) \cdot \nabla) \mathbf{u}_h^{i+1} \mathbf{v} \, dx}{|\mathbf{v}|_{1,\Omega}} + \sup_{\substack{q \in M \\ q \neq 0}} \frac{\int_{\Omega} q \operatorname{div} \mathbf{u}_h^{i+1} \, dx}{\|q\|_{L^2(\Omega)}} \right), \end{aligned} \tag{5.10}$$

where

$$\langle \mathcal{R}, \mathbf{v} - \mathbf{v}_h \rangle = \sum_{K \in \mathcal{T}_h} \left\{ \int_K (\mathbf{f}_h + \nu \Delta \mathbf{u}_h^{i+1} - (\mathbf{u}_h^i \cdot \nabla) \mathbf{u}_h^{i+1} - (\mathbf{u}_h^{i+1} \cdot \nabla) \mathbf{u}_h^i \right.$$

$$\begin{aligned}
 &+(\mathbf{u}_h^i \cdot \nabla) \mathbf{u}_h^i - \nabla p_h^{i+1})(\mathbf{v} - \mathbf{v}_h) \, d\mathbf{x} \\
 &-\frac{1}{2} \sum_{e \in \mathcal{E}_{K,\Omega}} \int_e \left[v \frac{\partial \mathbf{u}_h^{i+1}}{\partial n} - p_h^{i+1} \mathbf{n} \right] \cdot (\mathbf{v} - \mathbf{v}_h) \, d\tau \Big\}.
 \end{aligned}$$

Taking \mathbf{v}_h equal to the image $\mathcal{R}_h \mathbf{v}$ of \mathbf{v} by the Clément operator in (5.10), we obtain the desired estimate for $\|\mathbf{U} - \mathbf{U}_h^{i+1}\|_{X \times M}$.

□

We address now the efficiency of the previous indicators.

Theorem 5.2 *For each $K \in \mathcal{T}_h$, the following estimates hold for the indicators $\eta_{K,i}^{(L)}$ defined in (5.6)*

$$\eta_{K,i}^{(L)} \leq \| \mathbf{u} - \mathbf{u}_h^{i+1} \|_{1,K} + \| \mathbf{u} - \mathbf{u}_h^i \|_{1,K}, \tag{5.11}$$

and for the indicators $\eta_{K,i}^{(D)}$ defined in (5.7)

$$\eta_{K,i}^{(D)} \leq C \left(\eta_{K,i}^{(L)} + \| \mathbf{u} - \mathbf{u}_h^{i+1} \|_{1,\omega_K} + \| p_h^{i+1} - p \|_{L^2(\omega_K)} + \sum_{\kappa \subset \omega_K} h_\kappa \| \mathbf{f} - \mathbf{f}_h \|_{L^2(\kappa)} \right), \tag{5.12}$$

where ω_K is the union of the elements sharing at least one edge with K .

Proof The estimation of the linearization indicator follows easily from the triangle inequality by introducing \mathbf{u} in $\eta_{K,i}^{(L)}$. We now estimate the discretization indicator $\eta_{K,i}^{(D)}$. We proceed in two steps:

(i) We start by taking $\mathbf{v}_h = 0$ and by adding and subtracting $\int_\Omega (\mathbf{u}_h^{i+1} \cdot \nabla) \mathbf{u} \mathbf{v} \, d\mathbf{x}$ in (5.3). We obtain

$$\begin{aligned}
 &\sum_{K \in \mathcal{T}_h} \left(\int_K (\mathbf{f}_h + v \Delta \mathbf{u}_h^{i+1} - (\mathbf{u}_h^i \cdot \nabla) \mathbf{u}_h^{i+1} - (\mathbf{u}_h^{i+1} \cdot \nabla) \mathbf{u}_h^i + (\mathbf{u}_h^i \cdot \nabla) \mathbf{u}_h^i - \nabla p_h^{i+1}) \mathbf{v} \right) d\mathbf{x} \\
 &= v \int_\Omega \nabla (\mathbf{u} - \mathbf{u}_h^{i+1}) \nabla \mathbf{v} \, d\mathbf{x} + \int_\Omega ((\mathbf{u} - \mathbf{u}_h^{i+1}) \cdot \nabla) \mathbf{u} \mathbf{v} \, d\mathbf{x} - \sum_{K \in \mathcal{T}_h} \int_K (\mathbf{f} - \mathbf{f}_h) \mathbf{v} \, d\mathbf{x} \\
 &+ \frac{1}{2} \sum_{e \in \mathcal{E}_{K,\Omega}} \int_e \left[\frac{\partial \mathbf{u}_h^{i+1}}{\partial n} - p_h^{i+1} \mathbf{n} \right] \cdot \mathbf{v} \, d\tau \Big\} + \int_\Omega (\mathbf{u}_h^{i+1} \cdot \nabla) (\mathbf{u} - \mathbf{u}_h^{i+1}) \mathbf{v} \, d\mathbf{x} \\
 &+ \int_\Omega ((\mathbf{u}_h^{i+1} - \mathbf{u}_h^i) \cdot \nabla) \mathbf{u}_h^{i+1} \mathbf{v} \, d\mathbf{x} + \int_\Omega ((\mathbf{u}_h^i - \mathbf{u}_h^{i+1}) \cdot \nabla) \mathbf{u}_h^i \mathbf{v} \, d\mathbf{x} + \int_\Omega (p_h^{i+1} - p) \operatorname{div} \mathbf{v} \, d\mathbf{x}.
 \end{aligned} \tag{5.13}$$

We choose $\mathbf{v} = \mathbf{v}_K$ such that

$$\mathbf{v}_K = \begin{cases} (\mathbf{f}_h + v \Delta \mathbf{u}_h^{i+1} - (\mathbf{u}_h^i \cdot \nabla) \mathbf{u}_h^{i+1} - \nabla p_h^{i+1}) b_K & \text{on } K \\ 0 & \text{on } \Omega \setminus K, \end{cases}$$

where b_K is the bubble function of the element K . We get the following equation:

$$\begin{aligned} & \sum_{K \in \mathcal{T}_h} \int_K (\mathbf{f}_h + \nu \Delta \mathbf{u}_h^{i+1} - (\mathbf{u}_h^i \cdot \nabla) \mathbf{u}_h^{i+1} - (\mathbf{u}_h^{i+1} \cdot \nabla) \mathbf{u}_h^i + (\mathbf{u}_h^i \cdot \nabla) \mathbf{u}_h^i - \nabla p_h^{i+1})^2 b_K \, dx \\ &= \nu \int_{\Omega} \nabla(\mathbf{u} - \mathbf{u}_h^{i+1}) \nabla \mathbf{v}_K \, d\mathbf{x} + \int_{\Omega} ((\mathbf{u} - \mathbf{u}_h^{i+1}) \cdot \nabla) \mathbf{u} \, \mathbf{v}_K \, d\mathbf{x} - \sum_{K \in \mathcal{T}_h} \int_K (\mathbf{f} - \mathbf{f}_h) \mathbf{v}_K \, d\mathbf{x} \\ &+ \int_{\Omega} (\mathbf{u}_h^{i+1} \cdot \nabla) (\mathbf{u} - \mathbf{u}_h^{i+1}) \mathbf{v}_K \, d\mathbf{x} + \int_{\Omega} ((\mathbf{u}_h^{i+1} - \mathbf{u}_h^i) \cdot \nabla) \mathbf{u}_h^{i+1} \mathbf{v}_K \, d\mathbf{x} \\ &+ \int_{\Omega} ((\mathbf{u}_h^i - \mathbf{u}_h^{i+1}) \cdot \nabla) \mathbf{u}_h^i \mathbf{v}_K \, d\mathbf{x} + \int_{\Omega} (p_h^{i+1} - p) \operatorname{div} \mathbf{v}_K \, d\mathbf{x}. \end{aligned} \tag{5.14}$$

By using Cauchy–Schwarz inequality, (5.1) and (5.2), we obtain the following estimate of the first term of the local discretization estimator $\eta_{K,i}^{(D)}$

$$\begin{aligned} & h_K \|\mathbf{f}_h + \nu \Delta \mathbf{u}_h^{i+1} - (\mathbf{u}_h^i \cdot \nabla) \mathbf{u}_h^{i+1} - (\mathbf{u}_h^{i+1} \cdot \nabla) \mathbf{u}_h^i + (\mathbf{u}_h^i \cdot \nabla) \mathbf{u}_h^i - \nabla p_h^{i+1}\|_{L^2(K)} \\ & \leq C \left(\|\mathbf{u} - \mathbf{u}_h^{i+1}\|_{1,K} + h_K \|\mathbf{f} - \mathbf{f}_h\|_{L^2(K)} + \|p_h^{i+1} - p\|_{L^2(\Omega)} + \eta_{K,i}^{(L)} \right). \end{aligned} \tag{5.15}$$

(ii) We now estimate the second term of $\eta_{K,i}^{(D)}$. Rewriting (5.13), we infer

$$\begin{aligned} & \frac{1}{2} \sum_{e \in \mathcal{E}_{K,\Omega}} \int_e \left[\frac{\partial \mathbf{u}_h^{i+1}}{\partial n} - p_h^{i+1} \mathbf{n} \right] \cdot \mathbf{v} \, d\tau \\ &= \int_K (\mathbf{f}_h + \nu \Delta \mathbf{u}_h^{i+1} - (\mathbf{u}_h^i \cdot \nabla) \mathbf{u}_h^{i+1} - (\mathbf{u}_h^{i+1} \cdot \nabla) \mathbf{u}_h^i + (\mathbf{u}_h^i \cdot \nabla) \mathbf{u}_h^i - \nabla p_h^{i+1}) \mathbf{v} \, d\mathbf{x} \\ &+ \nu \int_{\Omega} \nabla(\mathbf{u}_h^{i+1} - \mathbf{u}) \nabla \mathbf{v} \, d\mathbf{x} + \int_{\Omega} ((\mathbf{u}_h^{i+1} - \mathbf{u}) \cdot \nabla) \mathbf{u} \mathbf{v} \, d\mathbf{x} + \sum_{K \in \mathcal{T}_h} \int_K (\mathbf{f} - \mathbf{f}_h) \mathbf{v} \, d\mathbf{x} \\ &+ \int_{\Omega} (\mathbf{u}_h^{i+1} \cdot \nabla) (\mathbf{u}_h^{i+1} - \mathbf{u}) \mathbf{v} \, d\mathbf{x} + \int_{\Omega} ((\mathbf{u}_h^i - \mathbf{u}_h^{i+1}) \cdot \nabla) \mathbf{u}_h^{i+1} \mathbf{v} \, d\mathbf{x} \\ &+ \int_{\Omega} ((\mathbf{u}_h^{i+1} - \mathbf{u}_h^i) \cdot \nabla) \mathbf{u}_h^i \mathbf{v} \, d\mathbf{x} + \int_{\Omega} (p - p_h^{i+1}) \operatorname{div} \mathbf{v} \, d\mathbf{x}. \end{aligned} \tag{5.16}$$

We choose $\mathbf{v} = \mathbf{v}_e$ such that

$$\mathbf{v}_e = \begin{cases} L_{e,\kappa} \left(\left[\frac{\partial \mathbf{u}_h^{i+1}}{\partial n} - p_h^{i+1} \mathbf{n} \right] b_e \right) & \kappa \in \{K, K'\} \\ 0 & \text{on } \Omega \setminus (K \cup K') \end{cases}$$

where b_e is the edge-bubble function, K' denotes the other element of \mathcal{T}_h that share e with K and $L_{e,\kappa}$ is a lifting operator from e into κ mapping polynomials vanishing on ∂e into polynomials vanishing in $\partial \kappa \setminus e$ and constructed from a fixed operator on the reference element (see Verfürth, [26]). Furthermore, we have for all $v \in P_r(e)$, the following properties

$$C \| v \|_{L^2(e)} \leq \| v b_e^{1/2} \|_{L^2(e)} \leq \| v \|_{L^2(e)}, \tag{5.17}$$

and

$$\| L_{e,\kappa} v \|_{L^2(\kappa)} + h_e |L_{e,\kappa} v|_{1,\kappa} \leq C h_e^{1/2} \| v \|_{L^2(e)}. \tag{5.18}$$

Using Cauchy–Schwarz inequality, (5.17) and (5.18) we get

$$\begin{aligned} & h_e^{1/2} \left\| \left[\frac{\partial \mathbf{u}_h^{i+1}}{\partial n} - p_h^{i+1} \mathbf{n} \right] \right\|_{L^2(e)}^2 \\ & \leq \left(v + \frac{2C}{v} \| \mathbf{f} \|_{0,\Omega} \right) \| \mathbf{u} - \mathbf{u}_h^{i+1} \|_{1,K \cup K'} \| \mathbf{v}_e \|_{L^2(e)} + h_e \| \mathbf{f} - \mathbf{f}_h \|_{L^2(K \cup K')} \| \mathbf{v}_e \|_{L^2(e)} \\ & \quad + h_e \| \mathbf{f}_h + v \Delta \mathbf{u}_h^{i+1} - (\mathbf{u}_h^i \cdot \nabla) \mathbf{u}_h^{i+1} - (\mathbf{u}_h^{i+1} \cdot \nabla) \mathbf{u}_h^i + (\mathbf{u}_h^i \cdot \nabla) \mathbf{u}_h^i - \nabla p_h^{i+1} \|_{L^2(K \cup K')} \| \mathbf{v}_e \|_{L^2(e)} \\ & \quad + \| p_h^{i+1} - p \|_{L^2(K \cup K')} \| \mathbf{v}_e \|_{L^2(e)} + \frac{2C}{v} \| \mathbf{f} \|_{0,\Omega} \eta_{K,i}^{(L)} \| \mathbf{v}_e \|_{L^2(e)}, \end{aligned} \tag{5.19}$$

with

$$\| \mathbf{v}_e \|_{L^2(e)} \leq c \left\| \left[v \frac{\partial \mathbf{u}_h^{i+1}}{\partial n} - p_h^{i+1} \mathbf{n} \right] \right\|_{L^2(e)}.$$

Thus, we have estimated the second term of the local discretization indicator $\eta_{K,i}^{(D)}$.

(iii) Finally, we take $q = q_K$ in (5.5) such that

$$q_K = \begin{cases} \operatorname{div} \mathbf{u}_h^{i+1} & \text{on } K \\ 0 & \text{on } \Omega \setminus K \end{cases}$$

We obtain

$$\| \operatorname{div} \mathbf{u}_h^{i+1} \|_{L^2(K)} \leq \| \mathbf{u} - \mathbf{u}_h^{i+1} \|_{1,K}. \tag{5.20}$$

Collecting the bounds above leads to the final result

$$\eta_{K,i}^{(D)} \leq C \left(\| \mathbf{u} - \mathbf{u}_h^{i+1} \|_{1,\omega_K} + \sum_{\kappa \subset \omega_K} h_\kappa \| \mathbf{f} - \mathbf{f}_h \|_{L^2(\kappa)} + \| p_h^{i+1} - p \|_{L^2(\omega_K)} + \eta_{K,i}^{(L)} \right).$$

□

Corollary 5.3 *If we use the following local stopping criteria (proceeding as in [11] or [13])*

$$\eta_{K,i}^{(L)} \leq \gamma_K \eta_{K,i}^{(D)}, \quad \forall K \in \mathcal{T}_h,$$

where γ_K is a positive parameter corresponding to the element K such that $\gamma_K C < 1$ (C is the constant of the previous theorem), we have

$$\eta_{K,i}^{(D)} \leq c \left(\| \mathbf{u} - \mathbf{u}_h^{i+1} \|_{1,\omega_K} + \| p_h^{i+1} - p \|_{L^2(\omega_K)} + \sum_{\kappa \subset \omega_K} h_\kappa \| \mathbf{f} - \mathbf{f}_h \|_{L^2(\kappa)} \right).$$

According to standard criteria, these estimates of the local linearization and discretization indicators are fully optimal [26]. In fact we observe that, up to the terms involving the data, the error is bounded by a constant times the sum of all indicators. As well, the indicators are bounded by the error in a neighborhood of K or e .

Instead the local stopping criteria introduced in the previous corollary, we can introduce a global one. In fact we introduce the global linearization error indicator $\eta_i^{(L)}$ and discretization error indicator $\eta_i^{(D)}$ defined by

$$\eta_i^{(L)} = \left(\sum_{K \in \mathcal{T}_h} (\eta_{K,i}^{(L)})^2 \right)^{1/2},$$

$$\eta_i^{(D)} = \left(\sum_{K \in \mathcal{T}_h} (\eta_{K,i}^{(D)})^2 \right)^{1/2}.$$

Corollary 5.4 *If we use the following global stopping criterion (proceeding as in [11] or [13])*

$$\eta_i^{(L)} \leq \gamma \eta_i^{(D)},$$

where γ is a positive parameter such that $\gamma C < 1$ (C is the constant of the previous theorem), we have

$$\eta_i^{(D)} \leq c \left(\| \mathbf{u} - \mathbf{u}_h^{i+1} \|_{1,\Omega} + \| \mathbf{u} - \mathbf{u}_h^i \|_{1,\Omega} + \| p_h^{i+1} - p \|_{L^2(\Omega)} + \sum_{K \subset \Omega} h_K \| \mathbf{f} - \mathbf{f}_h \|_{L^2(K)} \right).$$

6 Numerical results

In this section, we present numerical results for the Navier–Stokes Newton iterative algorithm (4.2) with the adaptive strategy and we compare with those obtained in [5] by the following modified fixed-point algorithm:

$$\begin{aligned} \forall \mathbf{v}_h \in X_h, \quad & \nu \int_{\Omega} \nabla \mathbf{u}_h^{i+1} \nabla \mathbf{v}_h \, d\mathbf{x} + \int_{\Omega} (\tilde{\mathbf{u}}_h^i \cdot \nabla) \mathbf{u}_h^{i+1} \mathbf{v}_h \, d\mathbf{x} - \int_{\Omega} p_h^{i+1} \operatorname{div} \mathbf{v}_h \, d\mathbf{x} = (\mathbf{f}, \mathbf{v}_h), \\ \forall q_h \in M_h, \quad & \int_{\Omega} q_h \operatorname{div} \mathbf{u}_h^{i+1} \, d\mathbf{x} = 0, \end{aligned} \tag{6.1}$$

where

$$\tilde{\mathbf{u}}_h^i = \frac{\mathbf{u}_h^i + \tilde{\mathbf{u}}_h^{i-1}}{2}.$$

These simulations have been performed using the code FreeFem++ due to F. Hecht and O. Pironneau, see [18]. For the numerical results showed in this work, we consider the same numerical algorithm of adaptive mesh refinement given in [5] (p. 1048) where the initial guess \mathbf{u}_h^0 is the solution of the Stokes problem with corresponding boundary

conditions. We consider the same numerical tests treated in [5] and we show the advantages of Scheme (4.2) compared to (6.1).

6.1 First test case

We consider the square $\Omega =]0, 3[^2$ and $\nu = 1$. Each edge is divided into N equal segments so that Ω is divided into $2N^2$ triangles. We consider the theoretical solution $(\mathbf{u}, p) = (\text{rot } \psi, p)$ where ψ and p are defined as follows

$$\psi(x, y) = e^{-30((x-1)^2+(y-1)^2)},$$

$$p(x, y) = \cos\left(\frac{2\pi}{3}x\right) \cos\left(\frac{2\pi}{3}y\right).$$

In [5], we defined and tested two different global stopping criteria:

$$\eta_i^{(L)} \leq 10^{-5} \quad \text{Classical stopping criterion,} \quad (6.2)$$

and

$$\eta_i^{(L)} \leq \gamma \eta_i^{(D)} \quad \text{New stopping criterion,} \quad (6.3)$$

where γ is a positive parameter which balances the discretization and linearization errors. In [11, 13], the authors introduced the new stopping criterion (6.3) and showed their advantages compared to the classical one (6.2) in term of CPU time of computation. The comparison is investigated numerically by performing multiple numerical tests. It is also shown in [5, 11] that (6.3) can be a good criterion for the adaptive method. In [5], we consider $\gamma = 0.01$ for the fixed-point method applied to the Navier–Stokes equation and showed again numerically the advantages of (6.3). So, in this work we will consider the case of (6.3) for $\gamma = 0.01$ and will compare the results with those obtained in [5]

For the numerical results showed in this work, the initial mesh is the uniform mesh with $N = 10$. Figures 1, 2, 3 and 4 show the evolution of the mesh during the iterations. We remark that, from an iteration to another, the mesh is mainly refined in the region where the velocity takes its higher values.

Figures 5 and 6 present the numerical and the exact first component of the velocity for the mesh refinement of Figure 4. We observe that the numerical velocity and the exact velocity are visually similar.

In [5], we showed comparisons between the adaptive and the uniform methods for Scheme (6.1) and we present the advantages of the adapted mesh method. Here in this work, we present comparisons of adaptive method between the schemes (4.2) and (6.1) in term of precision and CPU time of computation. Hence, we show the advantages of the Newton method compared to the fixed-point method despite the conditional convergence of Newton's method. In fact, for the academic test considered in this section, Newton's algorithm (4.2) converges always. In the next Lid Driven cavity

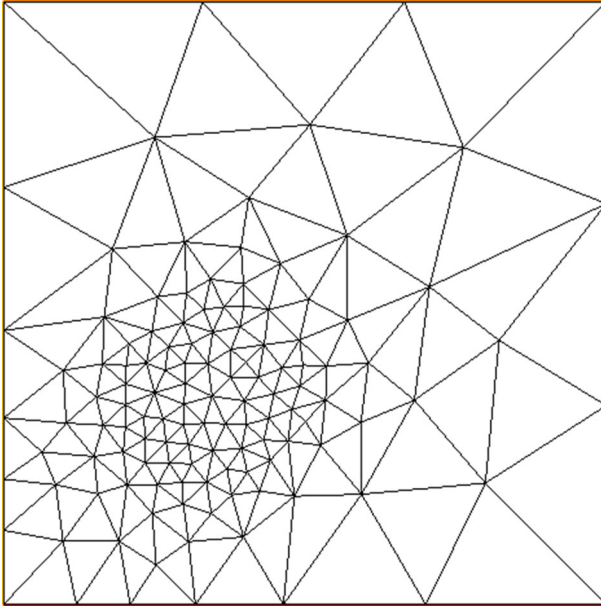


Fig. 1 273 vertices

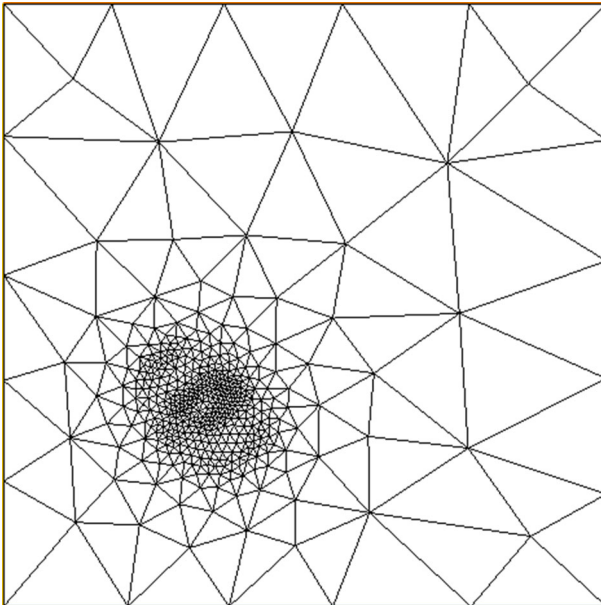


Fig. 2 507 vertices

test, the convergence depends on the initial guess \mathbf{u}_h^0 but we will show how we deal with this disadvantage.

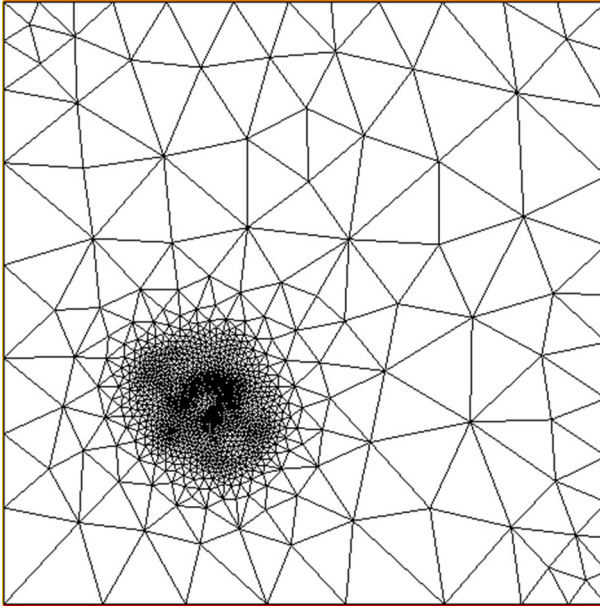


Fig. 3 891 vertices

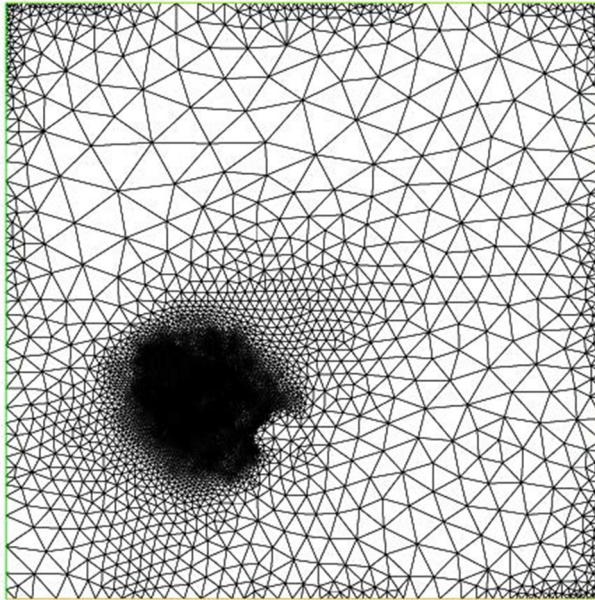


Fig. 4 1615 vertices

In Fig. 7, we show comparison in logarithmic scale of the error $E_r = \frac{|\mathbf{u} - \mathbf{u}_h|_{1,\Omega}}{|\mathbf{u}|_{1,\Omega}}$ versus the number of unknowns during the iterations. We remark that both methods

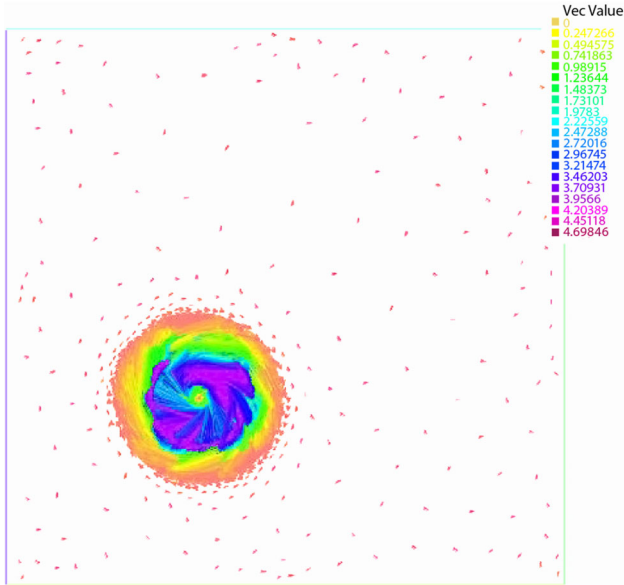


Fig. 5 Numerical velocity

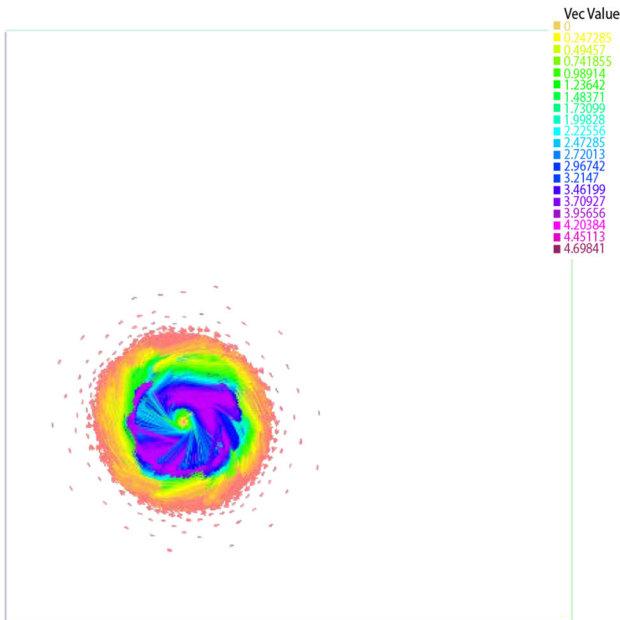


Fig. 6 Exact velocity

(Newton and fixed-point) give the same results. Figure 8 shows the iteration numbers during the refinement levels, as we can see, the Newton method is more efficient than the fixed-point method in term of numbers of iterations.

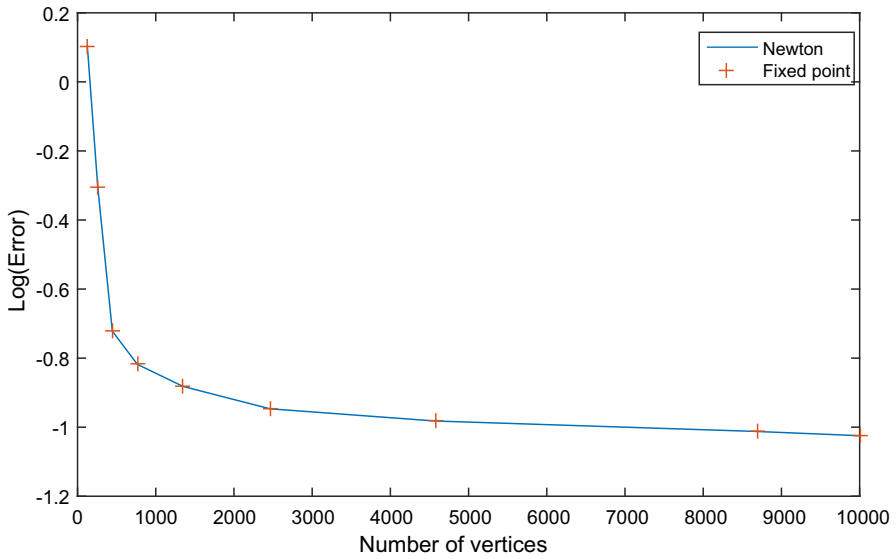


Fig. 7 E_r versus the global vertices number

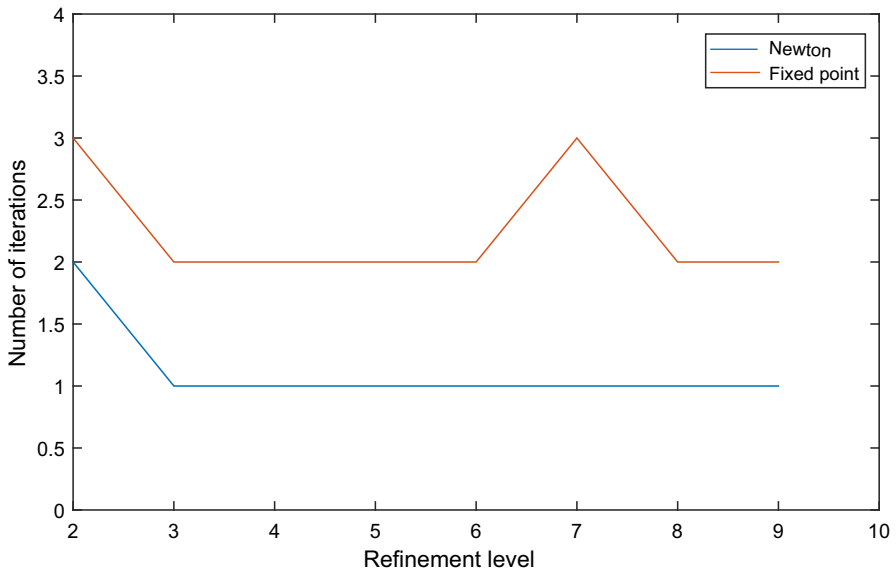


Fig. 8 Iterations number versus refinement level

To close the comparisons for this test, we show in Table 1 the CPU time of computation for each refinement level and for Newton and fixed-point methods. We remark that Newton’s method is slightly more effective than fixed-point’s method. In the next section and for the Lid Driven cavity test when the convergence is relatively slow, we will see clearly the efficiencies of Newton’s method in term of CPU time of computation.

Table 1 Comparison of the CPU time for Newton and fixed-point methods

Method	Refinement Level						
	3	4	5	6	7	8	9
Newton	1.45s	0.812s	1.419s	2.567s	4.84s	9.102s	11.493s
Fixed-point	1.537s	1.012s	1.789s	3.204s	7.868s	11.567s	14.1s

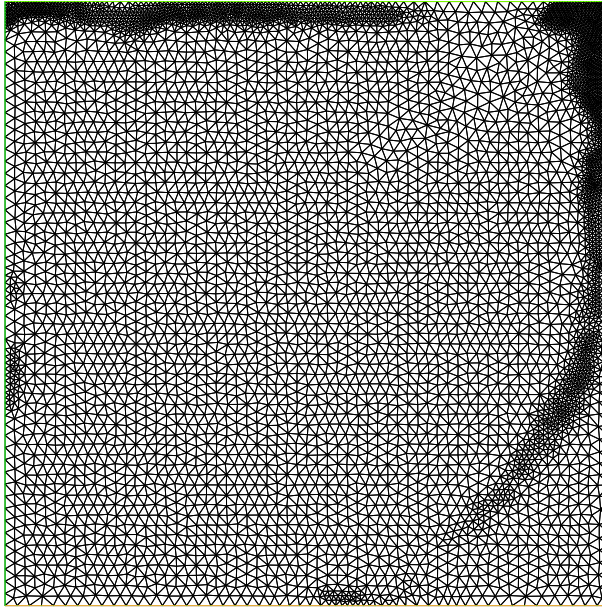


Fig. 9 Second refinement level ($Re = 9000$)

6.1.1 Second test case : Lid Driven cavity

In this section, we consider $\Omega =]0, 1[\times]0, 1[$, recall that $\nu = \frac{1}{Re}$ where Re is the Reynold number and complete the Navier–Stokes equations with the following boundary conditions: $\mathbf{u} = (1, 0)$ on the lid (top of Ω) and $\mathbf{u} = (0, 0)$ on the sides and the bottom of Ω .

In [5], we considered this same test called the Lid Driven Cavity and we cited several references working on this test case. In this work we will elaborate numerical results (and comparisons with [5]) using the adaptive mesh method and will give some numerical comparisons of the stream function ψ such that $\mathbf{u} = \mathbf{curl} \psi$ which verifies the following variational problem

$$\left\{ \begin{array}{l} \text{Find } \psi \in H_0^1(\Omega) \text{ such that for all } \phi \in H_0^1(\Omega) \text{ we have} \\ \int_{\Omega} \nabla \psi \nabla \phi = \int_{\Omega} \mathbf{curl} u \phi. \end{array} \right.$$

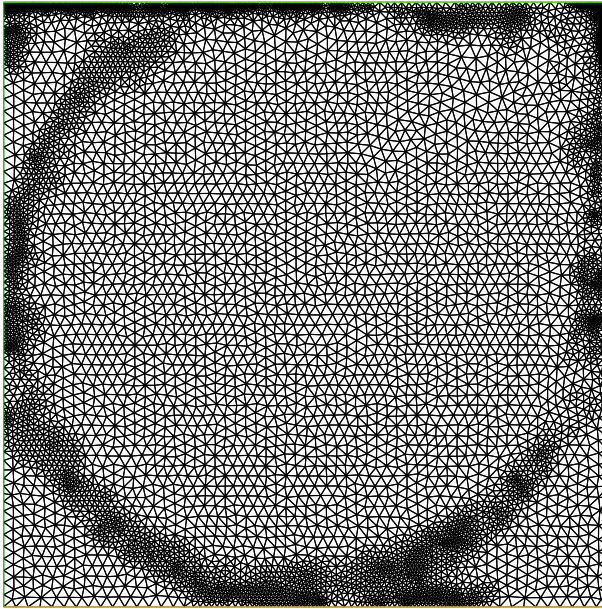


Fig. 10 Third refinement level ($Re = 9000$)

To compare with literature, we chose the finite elements of degree 2 for the velocity, of degree 1 for the pressure and of degree 2 for the stream function.

First of all, we begin by testing the Newton adaptive mesh algorithm corresponding to Scheme (4.2) for different values of Re and with a uniform initial mesh corresponding to $N = 30$. We remark that it diverges for $Re \geq 600$ while the fixed-point algorithm (6.1) converges for high Reynolds numbers (see [5]). In fact, it is well known that the convergence of the Newton method depends on the initial guess \mathbf{u}_h^0 . To overcome this disadvantage, we allow the adaptive algorithm to compute the solution with the fixed-point scheme (6.1) for the first refinement level and to continue with the Newton scheme (4.2) for the other refinement levels. So, the new adaptive Newton's method converges for high Reynolds numbers. In this work, we test the convergence up to $Re = 10,000$. According to [14], physically at high Reynolds numbers, two dimensional cavity flow does not exist and any study that considers a two dimensional flow at high Reynolds numbers, is dealing with a fictitious flow.

We consider the Newton adaptive mesh algorithm and we allow a maximum number of vertices up to 10,000. In this case, the algorithm refines in some regions of the domain and coarsens in other regions following the indicators. Figures 9 and 10 show the evolution of the mesh for the second and third refinement levels for $Re = 9000$. We remark that, the concentration of the refinement is on the top of the Lid where the velocity is imposed, in the two corner singularities and on the complex vorticity region (see [2]).

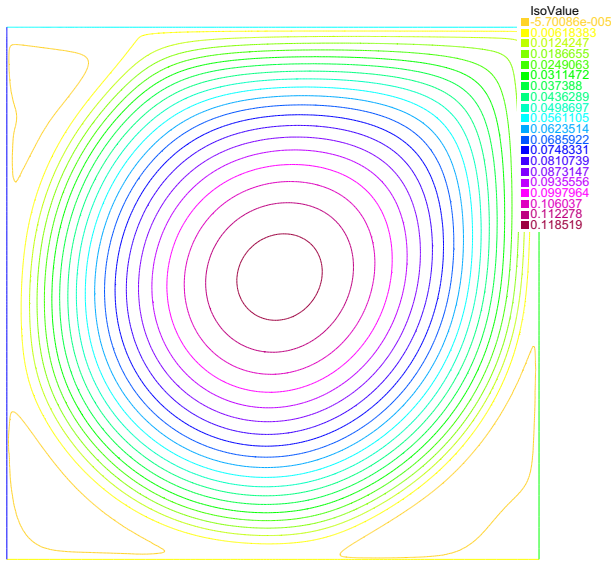


Fig. 11 Fixed point algorithm (Re = 9000)

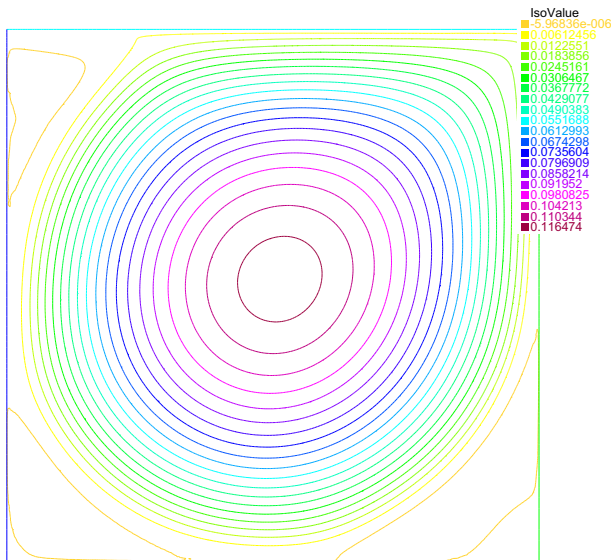


Fig. 12 Newton algorithm (Re = 9000)

Figures 11 and 12 show a comparison for $Re = 9000$ between the Newton adaptive algorithm (4.2) and the fixed-point adaptive algorithm (6.1). We can see that the figures are similar.

To show the efficiency of the proposed adaptive mesh method, we compare the adaptive mesh method with the literature. Table 2 shows the comparisons of $\| \psi \|_\infty$

Table 2 Comparison of $\|\psi\|_{L^\infty}$

Method	Reynold number				
	1000	2500	5000	7500	10,000
Fixed-point	0.1183	0.1203	0.1201	0.1212	0.1198
Newton	0.1181	0.1203	0.1207	0.1206	0.1203
Erturk et al. [15]	0.11894	0.12147	0.12223	0.12238	0.12239

Table 3 Comparison of the CPU time of computation

Method	Reynold number				
	1000	2500	5000	7500	10,000
Fixed-point	181.23 s	221.81 s	353.41 s	521.02 s	671.19 s
Newton	69.62 s	91.22 s	138.53 s	171.23 s	264.35 s

with literature. It shows that the results of the Newton and fixed-point methods are approximately the same, and close to the results presented in [15].

Table 3 shows comparison of the CPU time of computation between the Newton and fixed-point methods. We remark the advantage of Newton's method which is faster than the fixed-point one.

6.2 Conclusion

In this work we have derived a posteriori error estimates for the Newton method applied to the the Navier–Stokes equations. These estimates yield a fully computable upper bound which allows to distinguish the discretization and the linearization errors. We compare in this work the numerical results with those presented in [5] and show the advantages of the proposed method. In fact, it avoids performing an excessive number of iterations.

References

1. Adams, R.A.: Sobolev Spaces. Academic Press, Cambridge (1978)
2. Araya, R., Poza, A.H., Valentin, F.: On a hierarchical error estimator combined with a stabilized method for the Navier–Stokes equations. *Numer. Methods Partial Differ. Equ.* **28**, 782–806 (2012)
3. Babuška, I., Rheinboldt, W.C.: Error estimates for adaptive finite element computations. *SIAM J. Numer. Anal.* **4**, 736–754 (1978)
4. Baker, A., Dougalis, V.A., Karakashian, O.A.: On a higher order accurate fully discrete Galerkin approximation to the Navier–Stokes equation. *Math. Comput.* **39**, 339–375 (1982)
5. Bernardi, C., Dakroub, J., Mansour, G., Sayah, T.: A posteriori analysis of iterative algorithms for Navier–Stokes Problem. *ESIAM Math. Modell. Numer. Anal.* **50**(4), 1035–1055 (2016)
6. Bernardi, C., Hecht, F., Verfürth, R.: A finite element discretization of the three-dimensional Navier–Stokes equations with mixed boundary conditions. *ESAIM Math. Modell. Numer. Anal.* **43**(6), 1185–1201 (2009)
7. Bruneau, C.H., Saad, M.: The 2D lid-driven cavity problem revisited. *Comput. Fluids* **35**, 326–348 (2006)

8. Chaillou, A.L., Suri, M.: Computable error estimators for the approximation of nonlinear problems by linearized models. *Comput. Methods Appl. Mech. Eng.* **196**, 210–224 (2006)
9. Chaillou, A.L., Suri, M.: A posteriori estimation of the linearization error for strongly monotone nonlinear operators. *Comput. Methods Appl. Mech. Eng.* **205**, 72–87 (2007)
10. El Akkad, A., El Khalfi, A., Guessous, N.: An a posteriori estimate for mixed finite element approximations of the Navier–Stokes equations. *J. Korean Math. Soc.* **48**, 529–550 (2011)
11. El Alaoui, L., Ern, A., Vohralík, M.: Guaranteed and robust a posteriori error estimates and balancing discretization and linearization errors for monotone nonlinear problems. *Comput. Methods Appl. Mech. Eng.* **200**, 2782–2795 (2011)
12. Elman, H.C., Loghin, D., Wathen, A.J.: Preconditioning techniques for Newton’s method for the incompressible Navier–Stokes equations. *BIT Numer. Math.* **43**, 961–974 (2003)
13. Ern, A., Vohralík, M.: Adaptive inexact Newton methods with a posteriori stopping criteria for nonlinear diffusion PDEs. *SIAM J. Sci. Comput.* **35**(4), A1761–A1791 (2013)
14. Erturk, E.: Discussions on driven cavity flow. *Int. J. Numer. Methods Fluids* **60**, 747–774 (2009)
15. Erturk, E., Corke, T.C., Gokcol, C.: Numerical solutions of 2-D steady incompressible driven cavity flow at high Reynolds numbers. *Int. J. Numer. Methods Fluids* **48**, 747–774 (2005)
16. Ervin, V., Layton, W., Maubach, J.: A posteriori error estimators for a two-level finite element method for the Navier–Stokes equations. I.C.M.A. Technical Report, University of Pittsburgh (1995)
17. Girault, V., Raviart, P.A.: *Finite Element Methods for Navier–Stokes Equations*. Springer, Berlin (1986)
18. Hecht, F.: New development in FreeFem++. *J. Numer. Math.* **20**, 251–266 (2012)
19. Jin, H., Prudhomme, S.: A posteriori error estimation in finite element analysis. *Comput. Methods Appl. Mech. Eng.* **159**, 19–48 (1998)
20. John, V.: Residual a posteriori error estimates for two-level finite element methods for the Navier–Stokes equations. *Appl. Numer. Math.* **37**, 501–518 (2001)
21. Kim, S.D., Lee, Y.H., Shin, B.C.: Newton’s method for the Navier–Stokes equations with finite-element initial guess of stokes equations. *Comput. Math. Appl.* **51**(5), 805–816 (2006)
22. Pironneau, O.: *Méthodes des éléments finis pour les fluides*, Collection Recherches en Mathématiques Appliquées, vol. 7. Masson, Paris (1988)
23. Pousin, J., Rappaz, J.: Consistency, stability, a priori and a posteriori errors for Petrov–Galerkin methods applied to nonlinear problems. *Numer. Math.* **69**(2), 213–231 (1994)
24. Prudhomme, S., Oden, J.T.: Residual a posteriori error estimates for two-level finite element methods for the Navier–Stokes equations. *Finite Elem. Anal. Des.* **33**, 247–262 (1999)
25. Sheu, T.W.H., Lin, R.K.: Newton linearization of the incompressible Navier–Stokes equations. *Int. J. Numer. Methods Fluids* **44**(3), 297–312 (2004)
26. Verfürth, R.: *A Posteriori Error Estimation Techniques For Finite Element Methods*. Numerical Mathematics and Scientific Computation. Academic Press, Oxford (2013)

Publisher’s Note Springer Nature remains neutral with regard to jurisdictional claims in published maps and institutional affiliations.